

## Radioactive Gamma-Ray Lines from Long-lived Neutron Star Merger Remnants

MENG-HUA CHEN,<sup>1</sup> LI-XIN LI,<sup>1</sup> AND EN-WEI LIANG<sup>2</sup>

<sup>1</sup>*Kavli Institute for Astronomy and Astrophysics, Peking University, Beijing 100871, China*

<sup>2</sup>*Guangxi Key Laboratory for Relativistic Astrophysics, School of Physical Science and Technology, Guangxi University, Nanning 530004, China*

### ABSTRACT

The observation of a kilonova AT2017gfo associated with the gravitational wave event GW170817 provides the first strong evidence that neutron star mergers are dominant contributors to the production of heavy  $r$ -process elements. Radioactive gamma-ray lines emitted from neutron star merger remnants provide a unique probe for investigating the nuclide composition and tracking its evolution. In this work, we studied the gamma-ray line features arising from the radioactive decay of heavy nuclei in the merger remnants based on the  $r$ -process nuclear reaction network and the astrophysical inputs derived from numerical relativity simulations. The decay chain of  $^{126}_{50}\text{Sn}$  ( $T_{1/2} = 230$  kyr)  $\rightarrow$   $^{126}_{51}\text{Sb}$  ( $T_{1/2} = 12.35$  days)  $\rightarrow$   $^{126}_{52}\text{Te}$  (stable) produces several bright gamma-ray lines with energies of 415, 667, and 695 keV, making it the most promising decay chain during the remnant phase. The photon fluxes of these bright gamma-ray lines reach  $\sim 10^{-5}$   $\gamma$  cm<sup>-2</sup> s<sup>-1</sup> for Galactic merger remnants with ages less than 100 kyr, which can be detected by the high energy resolution MeV gamma-ray detectors like the MASS mission.

*Keywords:* gamma-ray lines,  $r$ -process nucleosynthesis, neutron star mergers, kilonovae

### 1. INTRODUCTION

The rapid neutron-capture process ( $r$ -process) has long been considered responsible for the production of heavy elements beyond iron in the universe (Burbidge et al. 1957; Cowan et al. 2021). Neutron-rich materials ejected from the merger of binary neutron stars or neutron star–black hole are ideal sites for  $r$ -process nucleosynthesis (Lattimer & Schramm 1974; Symbalisty & Schramm 1982). Li & Paczyński (1998) first proposed that the radioactive decay of freshly synthesized heavy elements can thermalize the merger ejecta, leading to a rapidly evolving thermal transient known as a “kilonova”. Subsequent studies included the  $r$ -process nuclear reaction network and found that kilonova emission is centered in the optical/near-infrared band (Metzger et al. 2010; Korobkin et al. 2012; Barnes & Kasen 2013; Kasen et al. 2013; Barnes et al. 2016; Metzger 2019). In the first binary neutron star merger event detected by the LIGO/Virgo collaboration (GW170817, Abbott et al. 2017a), a thermal transient source was observed (AT2017gfo, Abbott et al. 2017b; Arcavi et al. 2017; Coulter et al. 2017; Cowperthwaite et al. 2017; Drout et al. 2017; Evans et al. 2017; Kasen et al. 2017; Kasliwal et al. 2017; Pian et al. 2017; Shappee et al. 2017; Smartt et al. 2017). The light curve and colour evolution of AT2017gfo are consistent with theoretical predictions of the kilonova model, providing the first strong evidence in support of neutron star mergers as the dominant contributor to the production of heavy  $r$ -process elements in the Universe (Kasen et al. 2017; Hotokezaka et al. 2018; Chen et al. 2024).

The radioactive decay of heavy elements in the merger ejecta during the optically thin phase may also produce a gamma-ray transient accompanying the kilonova (Hotokezaka et al. 2016; Li 2019; Korobkin et al. 2020; Wang et al. 2020; Chen et al. 2021, 2022) and an MeV neutrino flash (Chen et al. 2023; An et al. 2023). Detecting radioactive

physcmh@pku.edu.cn (MHC)

lxl@pku.edu.cn (LXL)

lew@gxu.edu.cn (EWL)

gamma-ray photons from neutron star mergers can provide conclusive evidence for probing the nuclide composition and tracking its evolution. However, it is a great challenge to detect the radioactive gamma-ray emission during the kilonova phase. To convincingly observe radioactive gamma-ray lines generated by  $r$ -process elements, extremely nearby merger events and more sensitive MeV gamma-ray detectors are required (Chen et al. 2021, 2022). Wu et al. (2019) suggested that detecting gamma-ray lines produced by the radioactive decay of long-lived heavy nuclei during the remnant phase within the Milky Way is the most promising strategy in the near-term. In this work, we included the  $r$ -process nuclear reaction network and the astrophysical inputs derived from numerical relativity simulations to further investigate the gamma-ray line features generated by the radioactive decay of long-lived nuclei in the merger remnants.

According to the neutron star merger rate inferred from the LIGO/Virgo gravitational wave detectors, the occurrence rate of such mergers within the Milky Way ranges between  $\sim 10$  and  $\sim 100 \text{ Myr}^{-1}$  (Chen et al. 2024). Therefore, the age of young neutron star merger remnants in our Galaxy typically falls between  $\sim 10$  and  $\sim 100 \text{ kyr}$ . To detect the radioactive gamma-ray line from merger remnants at this typical age, the heavy nucleus  $^{126}_{50}\text{Sn}$  with a half-life of 230 kyr is the most promising heavy element. On one hand,  $^{126}_{50}\text{Sn}$  resides close to the second  $r$ -process peak, where its production typically occurs at a high yield level. On the other hand, the gamma-ray energy released by the decay chain of  $^{126}_{50}\text{Sn}$  is  $\sim 2.8 \text{ MeV}$  per decay event, significantly higher than that of other heavy elements during the remnant phase. Moreover, a new MeV gamma-ray mission has recently been proposed, the MeV Astrophysical Spectroscopic Surveyor (MASS; Zhu et al. 2024). With its high line sensitivity in the MeV band, MASS is expected to a powerful instrument for gamma-ray line detection, providing an opportunity to detect radioactive gamma-ray line from merger remnants within the Milky way. In this work, we will focus on investigating the radioactive gamma-ray lines generated by  $^{126}_{50}\text{Sn}$  and explore their detectability by combining with the line sensitivity of MASS.

Radioactive gamma-ray lines produced by the long-lived nucleus  $^{126}_{50}\text{Sn}$  from the Galactic supernova remnants have been investigated by Qian et al. (1998). They assumed that supernovae are the sites of  $r$ -process nucleosynthesis. However, subsequent studies have revealed that supernovae are only capable of producing some of the lightest  $r$ -process elements (Arcones & Thielemann 2013; Wanajo 2013). Conversely, neutron star mergers are considered more ideal astrophysical sites for  $r$ -process nucleosynthesis, as confirmed by the observation of the kilonova AT2017gfo. The light curve and color evolution of AT2017gfo suggest that approximately  $0.05 M_{\odot}$  of heavy  $r$ -process elements were synthesized in the merger ejecta (Kasen et al. 2017; Chen & Liang 2024). Subsequent analysis of the observed spectrum further identified the presence of the heavy element strontium (Watson et al. 2019). Furthermore, heavy element tellurium (which resides at the second  $r$ -process peak) has been discovered in the kilonova associated with gamma-ray burst 230307A observed by James Webb Space Telescope (Levan et al. 2024). These observational results confirm that neutron star mergers are the dominant contributors to the production of heavy  $r$ -process elements (Chen et al. 2024).

This paper is organized as follows. In Section 2, we provide the details of  $r$ -process nucleosynthesis and describe the procedure used to calculate gamma-ray emission powered by the radioactive decay of  $r$ -process elements. Section 3 presents the results of radioactive gamma-ray emission from neutron star merger remnants. Conclusions and discussions are presented in Section 4.

## 2. METHODS

### 2.1. Nucleosynthesis

We use the nuclear reaction network code SkyNet for  $r$ -process nucleosynthesis simulations (Lippuner & Roberts 2017). The network includes 7843 nuclide species and  $\sim 1.4 \times 10^5$  nuclear reactions. The nuclear reaction rates used in SkyNet are taken from the JINA REACLIB database (Cyburt et al. 2010). Nuclear masses and radioactive decay data are obtained from AME2020 (Wang et al. 2021) and NUBASE2020 (Kondev et al. 2021), respectively. For nuclide species lacking experimental data, we use theoretical data derived from the Finite-Range Droplet Model (Möller et al. 2016). Neutron capture rates are calculated using the Hauser-Feshbach statistical code TALYS (Goriely et al. 2008). Nuclear fission processes are calculated using fission barriers from Möller et al. (2015) and fission fragment distributions from Kodama & Takahashi (1975). Gamma-ray radiation data of unstable nuclei are taken from the Evaluated Nuclear Data File library (ENDF/B-VIII.0: Brown et al. 2018).

Astrophysical inputs for  $r$ -process nucleosynthesis calculations are in agreement with numerical relativity simulations provided by Radice et al. (2018). Table 1 lists the parameters used in our nucleosynthesis simulations. We selected four sets of astrophysical inputs derived from two different types of equation of state (EOS): BHB1p (representing a

**Table 1.** Astrophysical inputs for  $r$ -process nucleosynthesis simulations. Parameter values are consistent with numerical relativity simulations provided by [Radice et al. \(2018\)](#). Two different types of equation of state (EOS) were considered in our simulations: BHB1p (a stiffer EOS) and LS220 (a softer EOS). Nucleosynthesis inputs for binary neutron star mergers include electron fraction ( $Y_e$ ), specific entropy ( $s$ ), and expansion velocity ( $v$ ).

Model	EOS	$M_1 + M_2 (M_\odot)$	$Y_e$	$s (k_B)$	$v (c)$
BHB1p_M135135	BHB1p	1.35+1.35	0.16	20	0.18
BHB1p_M140140	BHB1p	1.40+1.40	0.14	17	0.20
LS220_M140140	LS220	1.40+1.40	0.15	17	0.17
LS220_M140120	LS220	1.40+1.20	0.16	13	0.20

‘stiffer’ EOS) and LS220 (representing a ‘softer’ EOS). Their electron fractions  $Y_e$  and specific entropies  $s$  are  $\sim 0.15$  and  $\sim 15 k_B$ , respectively. Despite numerical relativity studies showing that the electron fraction of ejected materials typically ranges from 0.05 to 0.30, heavy element yields are not highly sensitive to the value of  $Y_e$  in cases of extreme neutron richness ( $Y_e \lesssim 0.25$ ), especially for the heavy elements around the second  $r$ -process peak ([Lippuner & Roberts 2015](#)).

## 2.2. Gamma-Ray Emission

The abundance of a nuclide can be defined as

$$Y_i(t) = \frac{N_i(t)}{N_B(t)}, \quad (1)$$

where  $N_i(t)$  and  $N_B(t)$  are the total numbers of the  $i$ th nuclide species and baryons, respectively. The total gamma-ray luminosity powered by the radioactive decay of heavy elements in the neutron star merger remnants can be obtained by

$$L_{\text{tot}}(t) = M_{\text{ej}} N_A \sum_i \lambda_i Y_i(t) E_\gamma, \quad (2)$$

where  $N_A$  is the Avogadro’s number,  $M_{\text{ej}}$  is the mass value of ejected materials,  $\lambda_i$  is the decay rate of the  $i$ th nuclide,  $Y_i(t)$  is the corresponding abundance, and  $E_\gamma$  is the gamma-ray energy released by individual nuclear reaction.

To calculate the spectrum of gamma-ray emission, we divide the photon energy range of  $[10^{-3}, 10^1]$  MeV into 400 energy bins in logarithmic space. The gamma-ray luminosity in an energy bin  $[E_1, E_2]$  is given by

$$L(E, t) = M_{\text{ej}} N_A \sum_i \lambda_i Y_i(t) \sum_{E_1}^{E_2} E_\gamma. \quad (3)$$

The corresponding photon flux can be written as

$$F(E, t) = \frac{L(E, t)}{4\pi D^2}, \quad (4)$$

where  $D$  is the distance to the source. Following [Hotokezaka et al. \(2016\)](#), we consider that each gamma-ray line is convolved with a Gaussian distribution with a central value  $E_c$  and a width  $\Delta F$ , i.e.,

$$F(E) = \int F(E, t) G(E | E_c, \Delta F^2) \delta F, \quad (5)$$

where  $G(E | E_c, \Delta F^2)$  is the normalized Gaussian distribution. The width of the Gaussian profile is estimated by  $\Delta F = 2\sqrt{\ln 2} v_{\text{NSM}}/c$ , where  $v_{\text{NSM}}$  is the expansion velocity of neutron star merger remnants. For merger remnants aged 10 – 100 kyr, the expansion velocities are likely to lie between 100 and 3000 km s $^{-1}$  ([Korobkin et al. 2020](#)).

## 3. RESULTS

Figure 1 shows the time evolution of the abundance of the long-lived nucleus  $^{126}_{50}\text{Sn}$ . Due to its half-life of 230 kyr, the abundance of  $^{126}_{50}\text{Sn}$  remains at the level of  $10^{-4}$  for approximately 100 kyr. After  $\sim 100$  kyr, a significant amount of  $^{126}_{50}\text{Sn}$  decays via the  $\beta$ -decay chain  $^{126}_{50}\text{Sn}$  ( $T_{1/2} = 230$  kyr)  $\rightarrow$   $^{126}_{51}\text{Sb}$  ( $T_{1/2} = 12.35$  days)  $\rightarrow$   $^{126}_{52}\text{Te}$  (stable) to form stable

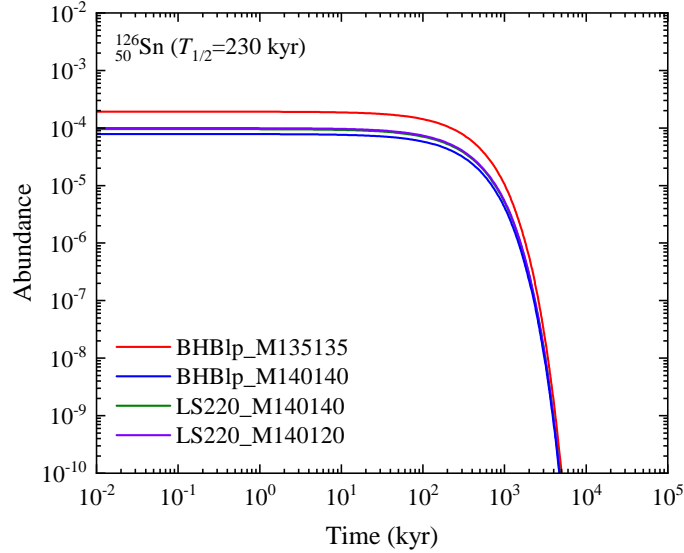


**Figure 1.** The time evolution of the abundance of long-lived nucleus  $^{126}_{50}\text{Sn}$  with a half-life of 230 kyr. Astrophysical inputs for  $r$ -process nucleosynthesis simulations are listed in Table 1.

element, leading to a dramatic decrease in the elemental abundance. Our calculations show that the variations in the abundance of the heavy nucleus  $^{126}_{50}\text{Sn}$  caused by different astrophysical inputs are within a factor of  $\sim 2$ . Note that the abundance of obtained through our detailed  $r$ -process simulations is broadly consistent with the initial abundance of  $^{126}_{50}\text{Sn}$  ( $Y_0 = 1.7 \times 10^{-4}$ ) used by Wu et al. (2019).

In Figure 2, we show the gamma-ray spectra generated by the radioactive decay of heavy nuclei from binary neutron star merger remnants at a time of  $t = 10$  kyr. The line sensitivities for MASS taken from Zhu et al. (2024) are also plotted for comparison. It is found that the energy of radioactive gamma-ray lines mainly ranges from 0.1 to 3 MeV, with specific energy fluxes between  $10^{-8}$  and  $10^{-5}$  MeV  $\text{cm}^{-2}$   $\text{s}^{-1}$ . The decay chain of  $^{126}_{50}\text{Sn}$  ( $T_{1/2} = 230$  kyr)  $\rightarrow$   $^{126}_{51}\text{Sb}$  ( $T_{1/2} = 12.35$  days)  $\rightarrow$   $^{126}_{52}\text{Te}$  (stable) produces more than 30 discrete gamma-ray lines, with a total gamma-ray energy release of approximately 2.8 MeV. The bright gamma-ray lines with a high intensity (probability of emitting a gamma-ray per decay greater than 80%) are 415 keV, 667 keV, and 695 keV. As seen in Figure 2, these bright radioactive gamma-ray lines can be detected by the MASS mission with an exposure time of  $10^7$  s.

To further study the features of gamma-ray emission produced by long-lived nuclei, we use the astrophysical model BHB1p\_M140140 as a representative case for our subsequent analysis. Figure 3 shows the radioactive gamma-ray spectra from neutron star merger remnants at times of 1 kyr, 10 kyr, and 100 kyr. As time goes on, the total gamma-ray flux produced by the merger remnants gradually decreases. The specific energy flux of several bright gamma-ray lines generated by the radioactive decay of  $^{126}_{51}\text{Sb}$  decreases from  $\sim 2 \times 10^{-5}$  to  $\sim 5 \times 10^{-6}$  MeV  $\text{cm}^{-2}$   $\text{s}^{-1}$  between 1 kyr and 100 kyr, decreasing by a factor of  $\sim 4$ . We further investigate the time evolution of photon fluxes of each bright gamma-ray line produced by heavy nucleus  $^{126}_{51}\text{Sb}$ , as shown in Figure 4. It is found that for neutron star merger remnants with ages less than 100 kyr, the radioactive gamma-ray lines generated by heavy element  $^{126}_{51}\text{Sb}$  can be detected by the MASS if the source is at a distance of 3 kpc. In other words, high energy resolution MeV gamma-ray detectors like MASS can identify young merger remnants ( $\lesssim 100$  kyr) within the Milky Way.

The nuclear physics inputs may affect the radioactive gamma-ray emission from neutron star merger remnants. To explore its sensitivity to the nuclear physics inputs, we estimate the radioactive gamma-ray spectrum using the Weizsäcker-Skyrme model provided by Wang et al. (2014), as shown in Figure 5. The merger remnant's age is 1 kyr and its distance is 10 kpc, consistent with the possible kilonova remnant associated with the guest star recorded in AD 1163 (Liu et al. 2019). One can observe that the radioactive gamma-ray spectrum calculated using the nuclear physics input derived from the Weizsäcker-Skyrme model has a similar total flux and global shape compared to that calculated using the Finite-Range Droplet model (Figure 2). Bright MeV gamma-ray lines generated by the radioactive decay of the heavy nucleus  $^{126}_{51}\text{Sb}$  can be identified in the gamma-ray spectrum. Our analysis further indicates that it is promising to use high energy resolution MeV gamma-ray detectors to observe these gamma-ray lines from Galactic kilonova remnants.

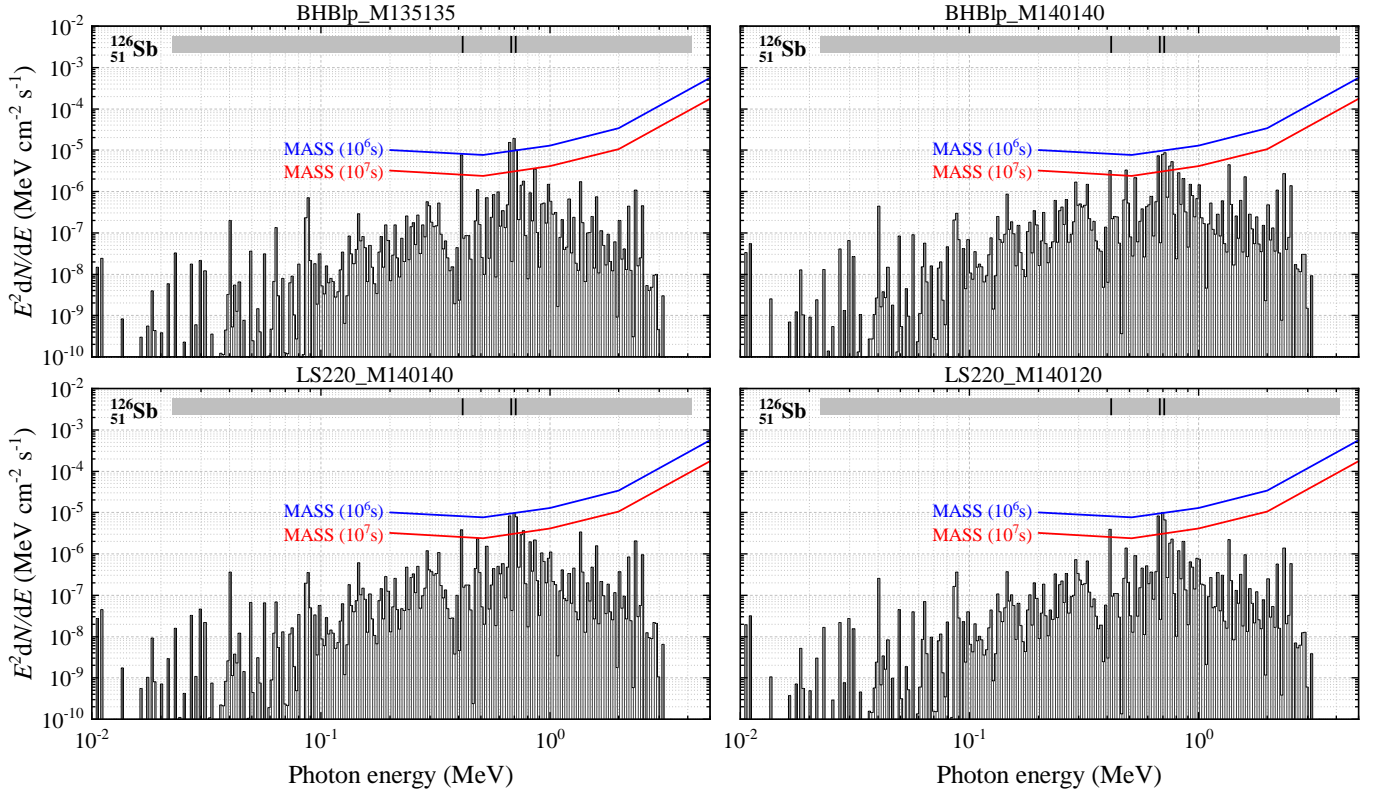


**Figure 2.** Radioactive gamma-ray lines from neutron star merger remnants with an age of 10 kyr. The ejected material from neutron star merger is set to  $0.01M_{\odot}$ . The distance to the source is 3 kpc. The line sensitivities with exposure times of  $10^6$  s (blue lines) and  $10^7$  s (red lines) for MASS taken from [Zhu et al. \(2024\)](#) are plotted for comparison. The bright gamma-ray lines generated by the radioactive decay of  $^{126}_{51}\text{Sb}$  are shown.

#### 4. SUMMARY AND DISCUSSION

Detection of radioactive gamma-ray photons emitted from neutron star mergers can provide direct evidence for probing the nuclide composition and tracking its evolution. In this study, we used the  $r$ -process nuclear reaction network and the astrophysical inputs derived from numerical relativity simulations to investigate the gamma-ray line features arising from the radioactive decay of long-lived nuclei in the merger remnants. Among these nuclei,  $^{126}_{50}\text{Sn}$ , with a half-life of 230 kyr, emerges as the most promising candidate. The abundance of heavy element  $^{126}_{50}\text{Sn}$  typically reaches a high level of  $\sim 10^{-4}$  within  $\sim 100$  kyr (Figure 1). Given such high yield, the decay chain of  $^{126}_{50}\text{Sn}$  ( $T_{1/2} = 230$  kyr)  $\rightarrow$   $^{126}_{51}\text{Sb}$  ( $T_{1/2} = 12.35$  days)  $\rightarrow$   $^{126}_{52}\text{Te}$  (stable) produces several bright gamma-ray lines with energies of 415, 667, and 695 keV (Figure 2 and Figure 3). The photon fluxes of these bright gamma-ray lines reach  $\sim 10^{-5}$   $\gamma$   $\text{cm}^{-2}$   $\text{s}^{-1}$  for neutron star merger remnants with ages less than 100 kyr, which can be detected if the source is at a distance of 3 kpc (Figure 4). This suggests that it is promising to use high energy resolution MeV gamma-ray detectors to observe gamma-ray lines generated by the radioactive decay of heavy  $r$ -process elements and to identify young neutron star merger remnants ( $\lesssim 100$  kyr) within the Milky Way. Our results are consistent with the analysis given by [Wu et al. \(2019\)](#). They suggested that  $^{126}_{50}\text{Sn}$  is the most promising nucleus for gamma-ray searches in neutron star merger remnants by investigating individual long-lived nuclei and assuming that each merger event contains a distribution of  $r$ -process nuclei following the Solar  $r$ -process abundances.

The event rate of binary neutron star merger inferred from the LIGO/Virgo gravitational wave detectors is  $\sim 1000$   $\text{Gpc}^{-3}$   $\text{yr}^{-1}$  ([Abbott et al. 2017a](#)). Assuming a local density of Milky Way-equivalent galaxies of  $\sim 0.01$   $\text{Mpc}^{-3}$ , the occurrence rate within our Galaxy is then  $\sim 100$   $\text{Myr}^{-1}$ . Thus, the age of the most recent Galactic merger remnant is estimated to be  $\sim 10$  kyr. However, it's worth noting that the youngest Galactic merger remnant could be substantially younger, with approximately a 10% probability of having an age less than 1 kyr. [Liu et al. \(2019\)](#) proposed that G4.8+6.2 is a possible kilonova remnant associated with the Korean guest star of AD 1163 in the Milky

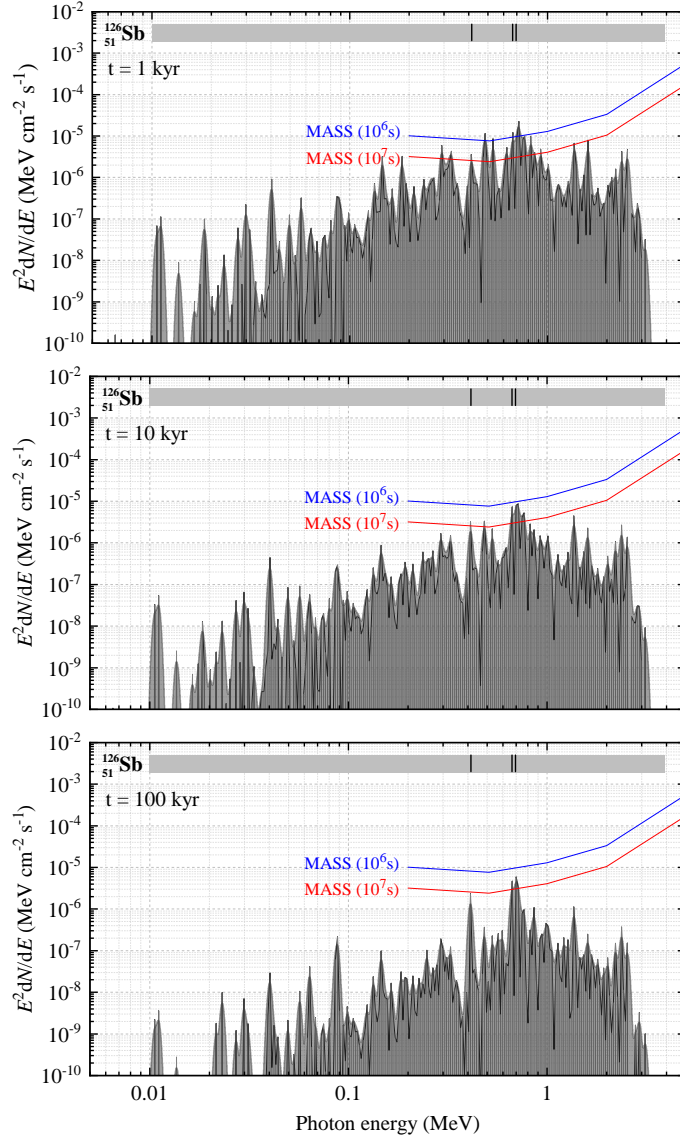


**Figure 3.** Radioactive gamma-ray spectra from neutron star merger remnants at times of 1 kyr (top panel), 10 kyr (middle panel), and 100 kyr (bottom panel). Here we take the astrophysical model BHBlp\_M140140 as a representative case for our analysis. The gray solid lines represent Gaussian broadening for the merger remnant with an expansion velocity of  $v_{\text{NSM}} = 3000 \text{ km s}^{-1}$ .

Way, with an age of  $\sim 1$  kyr. If G4.8+6.2 and AD 1163 are indeed associated, the radioactive gamma-ray emission lines produced by this kilonova remnant can be identified by MeV gamma-ray detectors (Figure 5).

The line sensitivity for the current gamma-ray mission INTEGRAL (Winkler et al. 2003) at 1 MeV is  $3 \times 10^{-5} \text{ } \gamma \text{ cm}^{-2} \text{ s}^{-1}$ , which is not sufficient to detect radioactive gamma-ray lines from long-lived neutron star merger remnants. Recently, Zhu et al. (2024) proposed a new MeV gamma-ray mission, the MeV Astrophysical Spectroscopic Surveyor (MASS). The MASS mission is a large area Compton telescope using 3D position sensitive CdZnTe detectors optimized for MeV gamma-ray line detection. The line sensitivities for the MASS mission could achieve  $1 \times 10^{-5}$  and  $4 \times 10^{-6} \text{ } \gamma \text{ cm}^{-2} \text{ s}^{-1}$  with exposure times of  $10^6$  and  $10^7$  seconds, respectively. With an energy resolution of 0.6% in the MeV band, MASS is sufficient to detect gamma-ray lines produced by the decay chain of  $^{126}_{50}\text{Sn}$  and to identify young Galactic kilonova remnants.

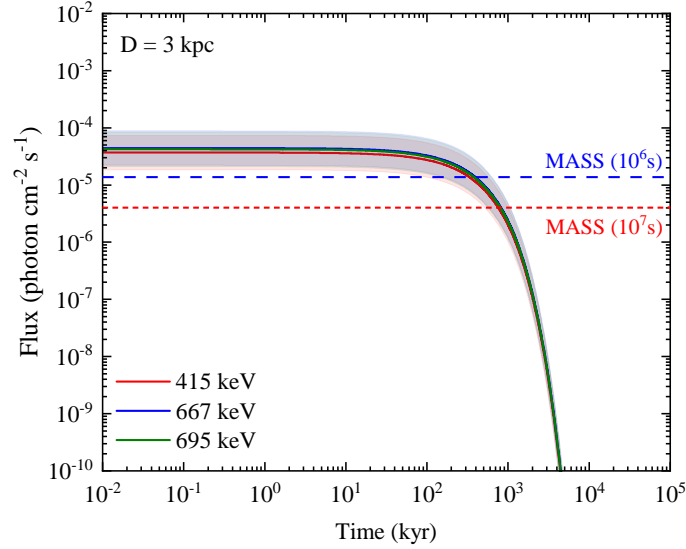


**Figure 4.** The time evolution of photon fluxes of gamma-ray lines generated by the radioactive decay of heavy nucleus  $^{126}_{51}\text{Sb}$ . The color shaded regions represent the possible range of photon flux caused by the astrophysical input models.

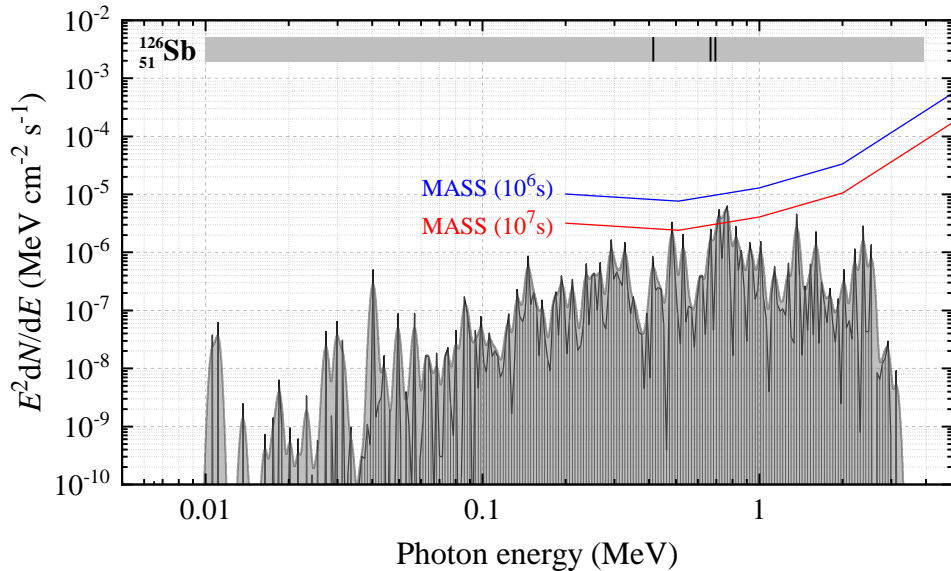


**Figure 5.** Radioactive gamma-ray spectra from neutron star merger remnants calculated using nuclear physics input derived from the Weizsäcker-Skyrme model provided by Wang et al. (2014). The nucleosynthesis inputs are consistent with the astrophysical model BHB1p.M140140 provided by Radice et al. (2018). The kilonova remnant’s age is 1 kyr, and its distance is 10 kpc, consistent with the possible kilonova remnant proposed by Liu et al. (2019). The gray solid lines indicate Doppler broadening caused by the expansion velocity of the merger remnant. The ejected material from the neutron star merger is set to  $0.01M_{\odot}$ .

We thank Hua Feng and Jia-Huan Zhu for valuable discussions. This work was supported by the National Natural Science Foundation of China (Grant Nos. 11973014, 12133003, and 12347172). MHC also acknowledges support from the China Postdoctoral Science Foundation (Grant Nos. GZB20230029 and 2024M750057). This work was also supported by the Guangxi Talent Program (Highland of Innovation Talents).

## ORCID iDs

Meng-Hua Chen: <https://orcid.org/0000-0001-8406-8683>

Li-Xin Li: <https://orcid.org/0000-0002-8466-321X>

En-Wei Liang: <https://orcid.org/0000-0002-7044-733X>

## REFERENCES

- Abbott, B. P., Abbott, R., Abbott, T. D., et al. 2017a, *PhRvL*, 119, 161101, doi: [10.1103/PhysRevLett.119.161101](https://doi.org/10.1103/PhysRevLett.119.161101)
- . 2017b, *ApJL*, 848, L12, doi: [10.3847/2041-8213/aa91c9](https://doi.org/10.3847/2041-8213/aa91c9)
- An, Y., Wu, M.-R., Guo, G., et al. 2023, *PhRvD*, 108, 123038, doi: [10.1103/PhysRevD.108.123038](https://doi.org/10.1103/PhysRevD.108.123038)
- Arcavi, I., Hosseinzadeh, G., Howell, D. A., et al. 2017, *Nature*, 551, 64, doi: [10.1038/nature24291](https://doi.org/10.1038/nature24291)
- Arcones, A., & Thielemann, F. K. 2013, *Journal of Physics G Nuclear Physics*, 40, 013201, doi: [10.1088/0954-3899/40/1/013201](https://doi.org/10.1088/0954-3899/40/1/013201)
- Barnes, J., & Kasen, D. 2013, *ApJ*, 775, 18, doi: [10.1088/0004-637X/775/1/18](https://doi.org/10.1088/0004-637X/775/1/18)
- Barnes, J., Kasen, D., Wu, M.-R., & Martínez-Pinedo, G. 2016, *ApJ*, 829, 110, doi: [10.3847/0004-637X/829/2/110](https://doi.org/10.3847/0004-637X/829/2/110)
- Brown, D. A., Chadwick, M. B., Capote, R., et al. 2018, *Nuclear Data Sheets*, 148, 1, doi: [10.1016/j.nds.2018.02.001](https://doi.org/10.1016/j.nds.2018.02.001)
- Burbidge, E. M., Burbidge, G. R., Fowler, W. A., & Hoyle, F. 1957, *Reviews of Modern Physics*, 29, 547, doi: [10.1103/RevModPhys.29.547](https://doi.org/10.1103/RevModPhys.29.547)
- Chen, M.-H., Hu, R.-C., & Liang, E.-W. 2022, *ApJL*, 932, L7, doi: [10.3847/2041-8213/ac7470](https://doi.org/10.3847/2041-8213/ac7470)
- . 2023, *MNRAS*, 520, 2806, doi: [10.1093/mnras/stad250](https://doi.org/10.1093/mnras/stad250)
- Chen, M.-H., Li, L.-X., Chen, Q.-H., Hu, R.-C., & Liang, E.-W. 2024, *MNRAS*, 529, 1154, doi: [10.1093/mnras/stae475](https://doi.org/10.1093/mnras/stae475)
- Chen, M.-H., Li, L.-X., Lin, D.-B., & Liang, E.-W. 2021, *ApJ*, 919, 59, doi: [10.3847/1538-4357/ac1267](https://doi.org/10.3847/1538-4357/ac1267)
- Chen, M.-H., & Liang, E.-W. 2024, *MNRAS*, 527, 5540, doi: [10.1093/mnras/stad3523](https://doi.org/10.1093/mnras/stad3523)
- Coulter, D. A., Foley, R. J., Kilpatrick, C. D., et al. 2017, *Science*, 358, 1556, doi: [10.1126/science.aap9811](https://doi.org/10.1126/science.aap9811)
- Cowan, J. J., Sneden, C., Lawler, J. E., et al. 2021, *Reviews of Modern Physics*, 93, 015002, doi: [10.1103/RevModPhys.93.015002](https://doi.org/10.1103/RevModPhys.93.015002)
- Cowperthwaite, P. S., Berger, E., Villar, V. A., et al. 2017, *ApJL*, 848, L17, doi: [10.3847/2041-8213/aa8fc7](https://doi.org/10.3847/2041-8213/aa8fc7)
- Cyburt, R. H., Amthor, A. M., Ferguson, R., et al. 2010, *ApJS*, 189, 240, doi: [10.1088/0067-0049/189/1/240](https://doi.org/10.1088/0067-0049/189/1/240)
- Drout, M. R., Piro, A. L., Shappee, B. J., et al. 2017, *Science*, 358, 1570, doi: [10.1126/science.aaq0049](https://doi.org/10.1126/science.aaq0049)
- Evans, P. A., Cenko, S. B., Kennea, J. A., et al. 2017, *Science*, 358, 1565, doi: [10.1126/science.aap9580](https://doi.org/10.1126/science.aap9580)
- Goriely, S., Hilaire, S., & Koning, A. J. 2008, *A&A*, 487, 767, doi: [10.1051/0004-6361:20078825](https://doi.org/10.1051/0004-6361:20078825)
- Hotokezaka, K., Beniamini, P., & Piran, T. 2018, *International Journal of Modern Physics D*, 27, 1842005, doi: [10.1142/S0218271818420051](https://doi.org/10.1142/S0218271818420051)
- Hotokezaka, K., Wanajo, S., Tanaka, M., et al. 2016, *MNRAS*, 459, 35, doi: [10.1093/mnras/stw404](https://doi.org/10.1093/mnras/stw404)
- Kasen, D., Badnell, N. R., & Barnes, J. 2013, *ApJ*, 774, 25, doi: [10.1088/0004-637X/774/1/25](https://doi.org/10.1088/0004-637X/774/1/25)
- Kasen, D., Metzger, B., Barnes, J., Quataert, E., & Ramirez-Ruiz, E. 2017, *Nature*, 551, 80, doi: [10.1038/nature24453](https://doi.org/10.1038/nature24453)
- Kasliwal, M. M., Nakar, E., Singer, L. P., et al. 2017, *Science*, 358, 1559, doi: [10.1126/science.aap9455](https://doi.org/10.1126/science.aap9455)
- Kodama, T., & Takahashi, K. 1975, *NuPhA*, 239, 489, doi: [10.1016/0375-9474\(75\)90381-4](https://doi.org/10.1016/0375-9474(75)90381-4)
- Kondev, F. G., Wang, M., Huang, W. J., Naimi, S., & Audi, G. 2021, *Chinese Physics C*, 45, 030001, doi: [10.1088/1674-1137/abddae](https://doi.org/10.1088/1674-1137/abddae)
- Korobkin, O., Rosswog, S., Arcones, A., & Winteler, C. 2012, *MNRAS*, 426, 1940, doi: [10.1111/j.1365-2966.2012.21859.x](https://doi.org/10.1111/j.1365-2966.2012.21859.x)
- Korobkin, O., Hungerford, A. M., Fryer, C. L., et al. 2020, *ApJ*, 889, 168, doi: [10.3847/1538-4357/ab64d8](https://doi.org/10.3847/1538-4357/ab64d8)
- Lattimer, J. M., & Schramm, D. N. 1974, *ApJL*, 192, L145, doi: [10.1086/181612](https://doi.org/10.1086/181612)
- Levan, A. J., Gompertz, B. P., Salafia, O. S., et al. 2024, *Nature*, 626, 737, doi: [10.1038/s41586-023-06759-1](https://doi.org/10.1038/s41586-023-06759-1)
- Li, L.-X. 2019, *ApJ*, 872, 19, doi: [10.3847/1538-4357/aaf961](https://doi.org/10.3847/1538-4357/aaf961)
- Li, L.-X., & Paczyński, B. 1998, *ApJL*, 507, L59, doi: [10.1086/311680](https://doi.org/10.1086/311680)
- Lippuner, J., & Roberts, L. F. 2015, *ApJ*, 815, 82, doi: [10.1088/0004-637X/815/2/82](https://doi.org/10.1088/0004-637X/815/2/82)
- . 2017, *ApJS*, 233, 18, doi: [10.3847/1538-4365/aa94cb](https://doi.org/10.3847/1538-4365/aa94cb)
- Liu, Y., Zou, Y.-C., Jiang, B., et al. 2019, *MNRAS*, 490, L21, doi: [10.1093/mnrasl/slz141](https://doi.org/10.1093/mnrasl/slz141)
- Metzger, B. D. 2019, *Living Reviews in Relativity*, 23, 1, doi: [10.1007/s41114-019-0024-0](https://doi.org/10.1007/s41114-019-0024-0)

- Metzger, B. D., Martínez-Pinedo, G., Darbha, S., et al. 2010, *MNRAS*, 406, 2650, doi: [10.1111/j.1365-2966.2010.16864.x](https://doi.org/10.1111/j.1365-2966.2010.16864.x)
- Möller, P., Sierk, A. J., Ichikawa, T., Iwamoto, A., & Mumpower, M. 2015, *PhRvC*, 91, 024310, doi: [10.1103/PhysRevC.91.024310](https://doi.org/10.1103/PhysRevC.91.024310)
- Möller, P., Sierk, A. J., Ichikawa, T., & Sagawa, H. 2016, *Atomic Data and Nuclear Data Tables*, 109, 1, doi: [10.1016/j.adt.2015.10.002](https://doi.org/10.1016/j.adt.2015.10.002)
- Pian, E., D'Avanzo, P., Benetti, S., et al. 2017, *Nature*, 551, 67, doi: [10.1038/nature24298](https://doi.org/10.1038/nature24298)
- Qian, Y. Z., Vogel, P., & Wasserburg, G. J. 1998, *ApJ*, 506, 868, doi: [10.1086/306285](https://doi.org/10.1086/306285)
- Radice, D., Perego, A., Hotokezaka, K., et al. 2018, *ApJ*, 869, 130, doi: [10.3847/1538-4357/aaf054](https://doi.org/10.3847/1538-4357/aaf054)
- Shappee, B. J., Simon, J. D., Drout, M. R., et al. 2017, *Science*, 358, 1574, doi: [10.1126/science.aag0186](https://doi.org/10.1126/science.aag0186)
- Smartt, S. J., Chen, T. W., Jerkstrand, A., et al. 2017, *Nature*, 551, 75, doi: [10.1038/nature24303](https://doi.org/10.1038/nature24303)
- Symbalisty, E., & Schramm, D. N. 1982, *Astrophys. Lett.*, 22, 143
- Wanajo, S. 2013, *ApJL*, 770, L22, doi: [10.1088/2041-8205/770/2/L22](https://doi.org/10.1088/2041-8205/770/2/L22)
- Wang, M., Huang, W. J., Kondev, F. G., Audi, G., & Naimi, S. 2021, *Chinese Physics C*, 45, 030003, doi: [10.1088/1674-1137/abddaf](https://doi.org/10.1088/1674-1137/abddaf)
- Wang, N., Liu, M., Wu, X., & Meng, J. 2014, *Physics Letters B*, 734, 215, doi: [10.1016/j.physletb.2014.05.049](https://doi.org/10.1016/j.physletb.2014.05.049)
- Wang, X., N3AS Collaboration, Vassh, N., et al. 2020, *ApJL*, 903, L3, doi: [10.3847/2041-8213/abbe18](https://doi.org/10.3847/2041-8213/abbe18)
- Watson, D., Hansen, C. J., Selsing, J., et al. 2019, *Nature*, 574, 497, doi: [10.1038/s41586-019-1676-3](https://doi.org/10.1038/s41586-019-1676-3)
- Winkler, C., Courvoisier, T. J. L., Di Cocco, G., et al. 2003, *A&A*, 411, L1, doi: [10.1051/0004-6361:20031288](https://doi.org/10.1051/0004-6361:20031288)
- Wu, M.-R., Banerjee, P., Metzger, B. D., et al. 2019, *ApJ*, 880, 23, doi: [10.3847/1538-4357/ab2593](https://doi.org/10.3847/1538-4357/ab2593)
- Zhu, J., Zheng, X., Feng, H., et al. 2024, *Experimental Astronomy*, 57, 2, doi: [10.1007/s10686-024-09920-4](https://doi.org/10.1007/s10686-024-09920-4)